

Advanced cancers: eradication in all cases using 3-bromopyruvate therapy to deplete ATP^{☆,☆☆}

Young H. Ko^{a,b,*}, Barbara L. Smith^a, Yuchuan Wang^a, Martin G. Pomper^a,
David A. Rini^c, Michael S. Torbenson^d, Joanne Hullihen^b, Peter L. Pedersen^{b,*}

^a The Russell H. Morgan Department of Radiology, Johns Hopkins University School of Medicine, Baltimore, MD 21205-2185, United States

^b Department of Biological Chemistry, Johns Hopkins University School of Medicine, Baltimore, MD 21205-2185, United States

^c Department of Art as Applied to Medicine, Johns Hopkins University School of Medicine, Baltimore, MD 21205-2185, United States

^d Department of Pathology, Johns Hopkins University School of Medicine, Baltimore, MD 21205-2185, United States

Received 25 August 2004

Available online 25 September 2004

Abstract

A common feature of many advanced cancers is their enhanced capacity to metabolize glucose to lactic acid. In a challenging study designed to assess whether such cancers can be debilitated, we seeded hepatocellular carcinoma cells expressing the highly glycolytic phenotype into two different locations of young rats. Advanced cancers (2–3 cm) developed and were treated with the alkylating agent 3-bromopyruvate, a lactate/pyruvate analog shown here to selectively deplete ATP and induce cell death. In all 19 treated animals advanced cancers were eradicated without apparent toxicity or recurrence. These findings attest to the feasibility of completely destroying advanced, highly glycolytic cancers.

© 2004 Elsevier Inc. All rights reserved.

Keywords: Advanced cancers; Liver/colon cancer; Cancer therapy; 3-Bromopyruvic acid; ATP depletion

Cancer is frequently asymptomatic reaching an advanced stage where treatment options are limited, e.g., liver cancer [1]. Significantly, such cancers frequently exhibit a highly glycolytic phenotype [2,3] dependent on the expression of hexokinase II [4]. In fact, it has been demonstrated that human liver cancers derived from metastatic colorectal cancer express enhanced levels of this enzyme [5]. Although the highly glycolytic phenotype has provided the basis for an emerging technique

for cancer detection [6], i.e., FDG-positron emission tomography, it has not been widely exploited as a therapeutic target with the mitochondria for facilitating ATP depletion and cancer destruction. Here, we report how advanced cancers can be selectively destroyed using this approach.

Materials and methods

Cell source, passage, culture, and viability or ATP content \pm 3-BrPA. A highly glycolytic hepatocellular carcinoma (HCC) line “AS-30D” [7,8] was used and maintained (Fig. 1A) in female Sprague–Dawley rats (Charles River). For culture, cells ($\sim 1 \times 10^6$) were seeded on a six-well plate in 2 ml RPMI 1640 medium (Invitrogen) containing 10% fetal bovine serum plus $1 \times$ antibiotic–antimycotic mixture (Invitrogen) at 37 °C for 3 h in a CO₂ incubator. Hepatocytes ($\sim 1.5 \times 10^6$) were fresh from Cambrex. Cell viability \pm 3-BrPA (Sigma) was monitored using the MTT assay (Sigma). For monitoring cell ATP levels, methods of culture using six-well plates and 3-BrPA treatment were as above. Then,

[☆] This work was supported by start-up funds to Y.H.K. from the Department of Radiology, by NIH Grants CA 10951 and CA 80118 to P.L.P. and Grant CA92871 to M.G.P.

^{☆☆} Abbreviations: 3-BrPA, 3-bromopyruvic acid; HCC, hepatocellular carcinoma; PET, positron emission tomography; FDG, ¹⁸F-2-deoxyglucose.

* Corresponding authors. Fax: +1 410 614 1944.

E-mail addresses: yko@jhmi.edu (Y.H. Ko), ppedersen@jhmi.edu (P.L. Pedersen).

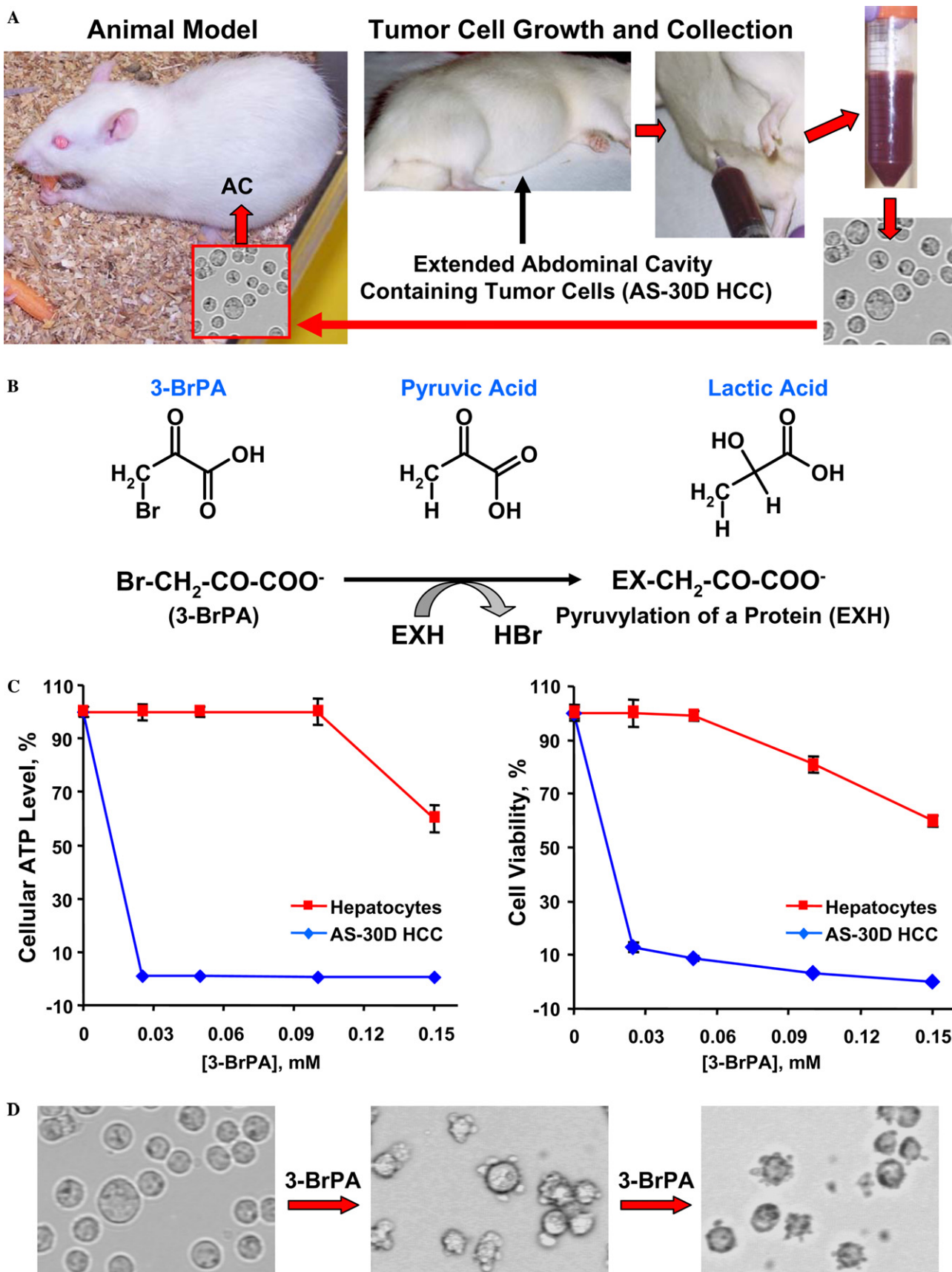


Fig. 1. HCC cells and 3-BrPA. (A) Growth and isolation of HCC cells (AS-30D). (B) Structure and chemical reactivity of 3-BrPA. (C) 3-BrPA-induced depletion of ATP in HCC cells (Left) and loss of viability (Right). (D) Intermediates (Center and Right) in the HCC death pathway.

100 μ l aliquots of cells, three for each of the six wells, were removed and transferred into wells of the white culture plate-96 (Perkin–Elmer). ATP was measured according to Perkin–Elmer using their cell lysate and ATPlite solutions, and Victor 1420 Multilabel Counter.

Induction of advanced cancers and therapy with 3-BrPA. Procedures adhered to Johns Hopkins University Animal Care and Use Committee guidelines. “Advanced cancer” is defined here in the rat as either a collection of HCC cells in the abdominal cavity that cause it to become extended (Fig. 1A) or a solid HCC of 2–3 cm (maximal dimension). To induce ascites tumor cell masses and abdominal tumors, 1 ml, $2-4 \times 10^7$ HCC cells was injected i.p. (Fig. 1A). This resulted in 5–6 days in ~ 40 ml ascites fluid filled with tumor cells (Fig. 1A), and where indicated, also in advanced spherical tumors 2–3 cm in diameter. To induce tumors in the upper back, 1 ml, $2-4 \times 10^7$ HCC cells was injected s.c. Non-spherical tumors of ~ 3 cm (maximal dimension) developed in about 7–10 days. Without treatment, rats hosting HCC cells in ascites form must be euthanized within 7–8 days and in solid form in about 14–21 days. For therapy, animals bearing tumor cells in the abdominal cavity, or together with a spherical tumor (2–3 cm diameter), were treated after 5–6 days with an i.p. injection of 1 ml freshly prepared 2.0 mM 3-BrPA in 1 \times PBS, pH 7.5, and then for 4 days with the same dosage. The animal named “Two Dottie” also received seven injections of 1 ml of 2.0 mM 3-BrPA on separate days at the tumor site. Those animals bearing tumors 1–2 cm (maximal dimension) in the upper back that were subjected to FDG PET prior to and following therapy were administered eight treatments on successive days with 1 ml of 2 mM 3-BrPA, also in 1 \times PBS, pH 7.5. Injection of 3-BrPA was into the tumor. The remaining animals containing large tumors (~ 3 cm maximal dimension) were treated on an individual basis depending on each tumor’s responsiveness to 3-BrPA (Table 1).

PET imaging. Rats fasted 12 h with water ad libitum were anesthetized i.p. with 75 mg/kg ketamine and 10 mg/kg xylazine (Abbott Park) in 100–200 μ l for induction and subjected to halothane (1% at 1 L/min). FDG (35.0 ± 12.7 MBq, 0.945 ± 0.342 mCi; range 32.7–57.7 MBq, 0.884–1.56 mCi) was injected in the tail vein (10–15 s bolus) in 150 μ l. After 45 min, rats were placed in the prone position on the platform of the scanner with the tumor placed within the field-of-view with the aid of

laser guidance. An ATLAS small animal PET scanner was used that has an 11.8 cm ring diameter scanner, an 8 cm aperture, a 6 cm effective transverse field-of-view, and a 2 cm axial field of view [9,10]. The imaging system comprised of 18 depth-of-interaction detector modules surrounds the rat. Radial and tangential resolutions of the reconstructed image (pixel size = 0.56 mm) were 1.36 mm at the center, 1.98 (radial), and 2.13 (tangential) at 2 cm radial offset. Sensitivity was $>2.0\%$ after correcting for positron escape. Maximal noise equivalent count rate was 10.3 kcps at 52.2 MBq (1.41 mCi) total activity for the rat phantom. These are comparable to those of the prototype scanner used in this study. Images were reconstructed by 3D OSEM [11]. No correction was made for attenuation or scatter. Regions of interest were drawn manually using ATLAS software to encompass the tumor and a region of equal size in the contralateral subcutaneous soft tissues (background). Tumor and background radioactivity were corrected for decay, injected dose, and animal weight, and were expressed in arbitrary units. A paired *t* test was performed using Microsoft Excel with Analyse-it. *P* values <0.05 were considered significant.

Histopathology. Tissues were fixed in 10% formalin, sliced at 5 mm intervals, and embedded in paraffin. Sections (4 μ m) were stained with hematoxylin and eosin.

Human equivalent of a rat tumor. Tumor location was determined by its position relative to the rat’s skeletal anatomy [12] and placed on the human figure using the corresponding skeletal landmarks. Its mass was evaluated by assessing the tumor to body size ratio in the rat and translating this to the human.

Results and discussion

The chemical agent 3-BrPA depletes ATP stores and inhibits HCC cell viability

For therapy, we selected the alkylating agent 3-BrPA [13]. This was based on the hypothesis that because of its

Table 1
History of animals in the advanced cancer treatment/survival study

Animal No.	Animal ID	Group ID	Tumor implantation site	Tumor development area	Method of treatment	Survival time (to date)
1	Star	1	AC	AC	IP	Alive (>1.3 year)
2	Tiny 9	1	AC	AC, LA	IP	(1.3 year)
3	Tip	1	AC	AC	IP	Alive (>1.3 year)
4	One Dottie	1	AC	AC, LA	IP	Alive (>7 months)
5	Two Dottie	1	AC	AC, LA	IP, D	Alive (>7 months)
6	Three Dottie	1	AC	AC, LA	IP	Alive (>7 months)
7 \rightarrow 12	C1 \rightarrow C6	1	AC	AC, LA	IP, saline (control)	6–7 days (euthanized)
13 \rightarrow 20	C7 \rightarrow C14	1	AC	AC	IP, saline (control)	6–7 days (euthanized)
21	B1	2	UB	UB, S	D, SC, IP	Alive (>7 months)
22	B2	2	UB	UB	D	Alive (>7 months)
23	B6	2	UB	UB, S	D, SC, IP	Alive (>7 months)
24	R1	2	UB	UB	D	Alive (>7 months)
25	R2	2	UB	UB, S	D	Alive (>7 months)
26	R3	2	UB	UB	D	Alive (>7 months)
27	R4	2	UB	UB, S	D, SC, IP	Alive (>7 month)
28	R6	2	UB	UB, S	D, SC	Alive (>7 months)
29 ^a	B3 ^a	2	UB	UB	D	Alive (>7 months)
30 ^a	B4 ^a	2	UB	UB	D	Alive (>7 months)
31 ^a	B5 ^a	2	UB	UB	D	Alive (>7 months)
32 ^a	R5 ^a	2	UB	UB	D	Alive (>7 months)
33	Sweetie	2	UB	UB	IP	Alive (>7 months)
34	Chubbet	2	None	None	None	Alive (>7 months)

Abbreviations used are: AC, abdominal cavity; LA, lower abdomen; UB, upper back; S, side; IP, intra-peritoneal; SC, subcutaneous; D, direct (locally); and ^aEmployed in PET imaging.

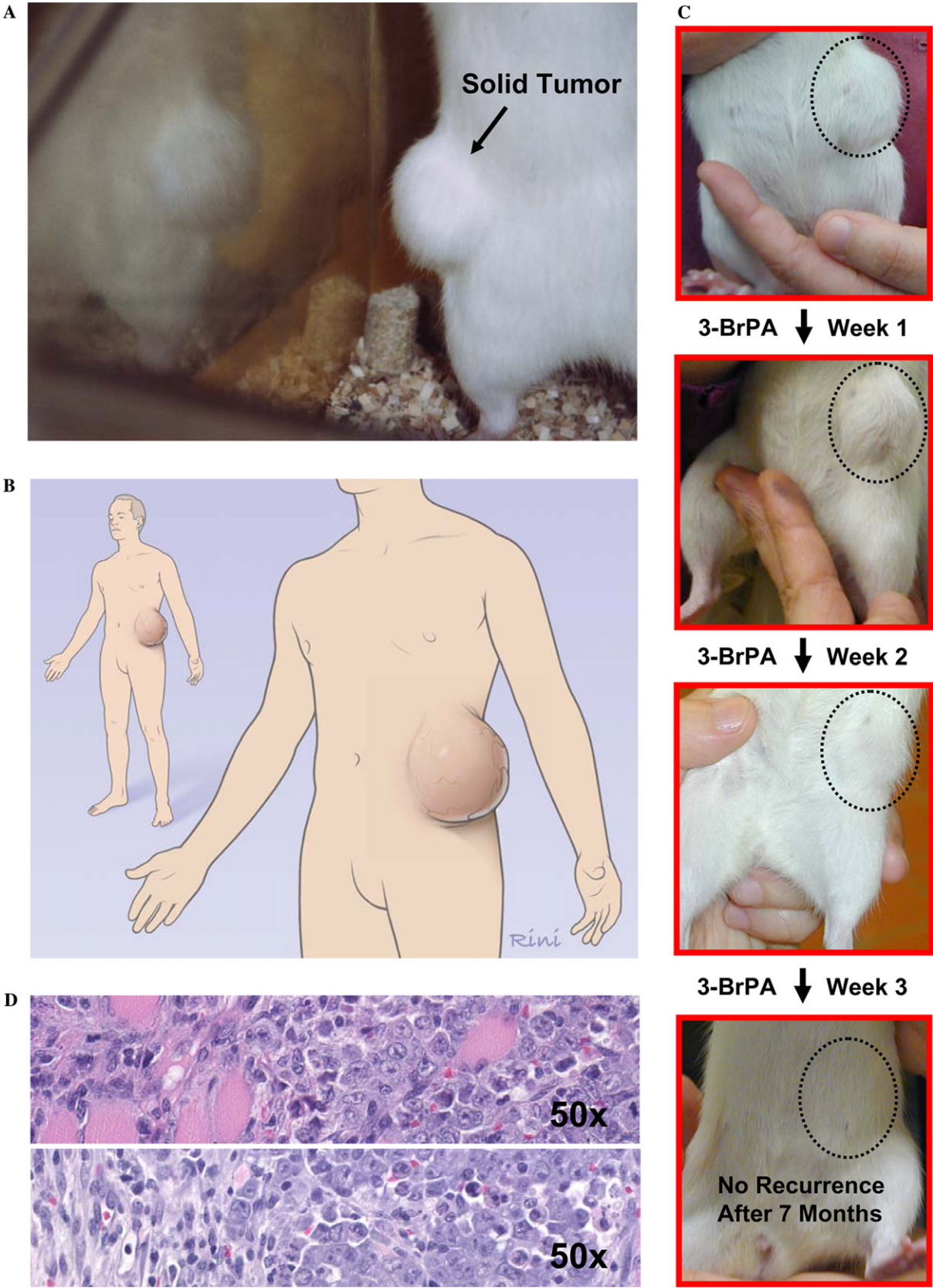


Fig. 2. Complete regression of an advanced abdominal tumor (HCC) after 3-BrPA Therapy. (A) Advanced HCC in “Two Dottie.” (B) Human equivalent. (C) Different treatment stages. (D) Tumor histopathology.

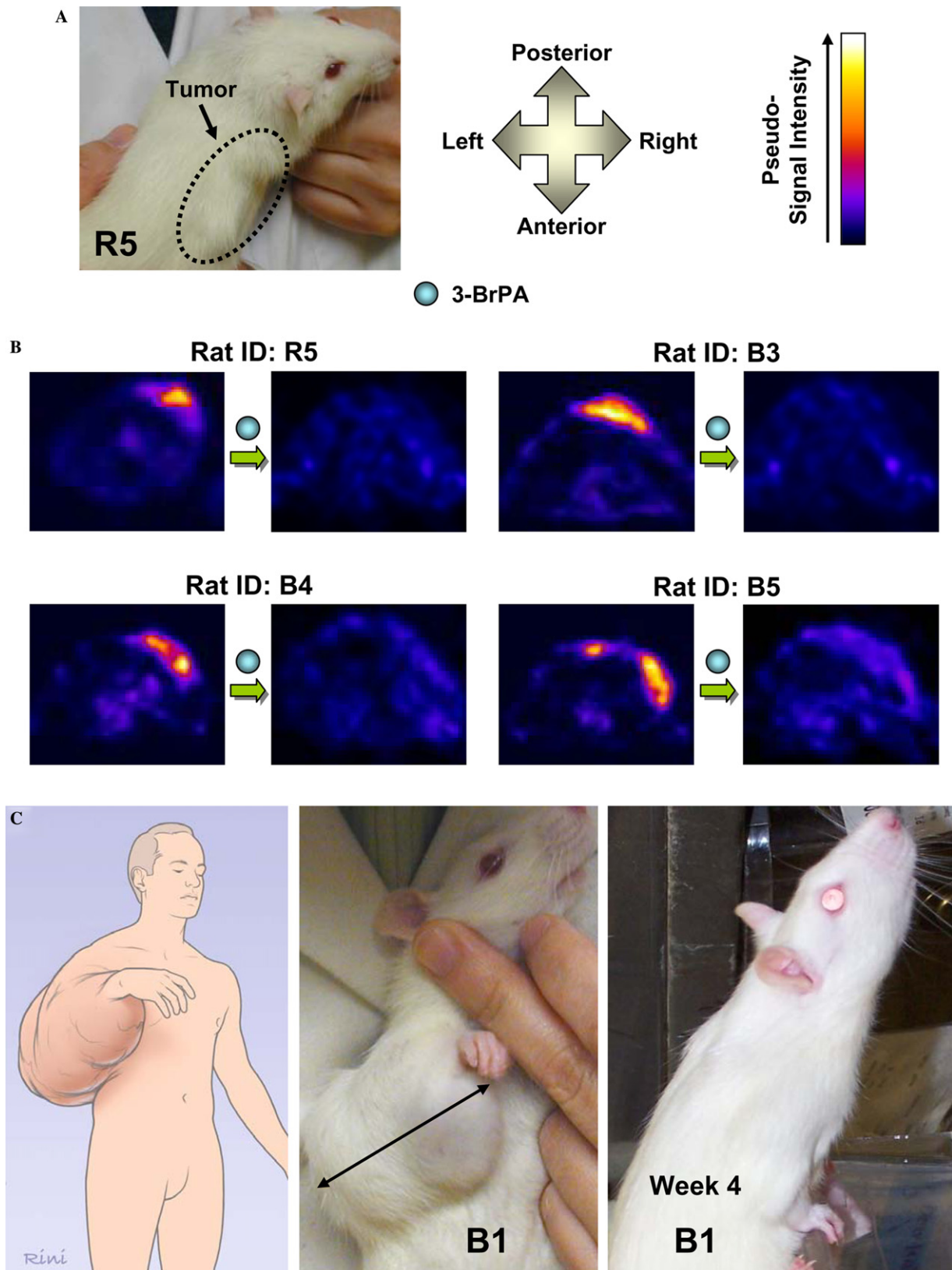


Fig. 3. (A) Preparation for FDG-PET. (Upper left) Rats R5, B3, B4, and B5 were allowed to develop tumors (HCCs). (Upper center) Positional designations for tumors. (Upper right) Pseudo-signal intensity bar. “yellow,” increased glucose consumption. (B) FDG-PET images of tumors on R5, B3, B4, and B5 Before and 12 days after 3-BrPA therapy. Therapy involved eight treatments. (C) Rat B1 as one example of nine rats each bearing an advanced tumor (~3 cm) eradicated by 3-BrPA therapy. (Center) Rat B1 bearing a large advanced tumor. (Left) Human equivalent. (Right) Rat B1 one week after 3 weeks of 3-BrPA therapy.

structural similarity to lactate (Fig. 1B), the reactive 3-BrPA may enter cancer cells on the same transporter that exports lactate and then induce ATP depletion. Although earlier work [14,15] showed that 3-BrPA inhibits in vitro the cell's two ATP producing systems, glycolysis and mitochondria, and has antitumor activity, the most critical support for the above hypothesis is presented in Figs. 1C and D. These data show directly that 3-BrPA induces ATP depletion and loss of HCC cell viability. In contrast, hepatocytes show resistance to 3-BrPA. These findings provided support for an ATP depletion-anticancer strategy (see also [Supplementary material](#)).

HCC cells growing internally in the abdominal cavity of test animals, and all advanced tumors (HCCs) projecting externally, regressed, and disappeared after 3-BrPA therapy

Table 1 provides information about the 34 female rats in this study divided into Groups 1 and 2. Group 1 animals, named “One Dottie,” “Two Dottie,” “Three Dottie,” “Tiny 9,” “Star,” and “Tip,” had their abdominal cavities filled with rapidly proliferating HCC cells, and the first four also had a spherical tumor (2–3 cm diameter) projecting from their lower abdomen. Fig. 2A shows “Two Dottie” facing her cage revealing the large tumor and its reflection while Fig. 2B presents the predicted human equivalent. “Two Dottie” and the other five animals were treated for five successive days with a single 3-BrPA injection/day into the abdominal cavity. Subsequently, “Two Dottie” also received seven injections on separate days at the tumor site. In 1 week, the extended abdomens regressed in all six animals and in 1 month the tumors completely disappeared. Fig. 2C summarizes the disappearance of the tumor in the abdomen of “Two Dottie.” These animals received no additional therapy and showed no tumor recurrence. With the exception of “Tiny Nine” who died tumor free 1.3 years after treatment, the remaining five animals are alive (Table 1). In contrast, all control animals (14 total), treated with saline rather than 3-BrPA, had to be euthanized after only 7–8 days. Histopathology of tumors derived there from showed tumor cell invasion into the abdominal wall (Fig. 2D) with two different cell morphologies, i.e., round and spindled (Fig. 2D).

Moderately advanced tumors (HCCs) growing in the upper backs of test animals also regressed and disappeared following therapy with 3-BrPA, a finding that correlated well with FDG-PET imaging

Results with Group 1 animals gave encouragement to apply 3-BrPA therapy to Group 2 animals bearing tumors in the upper back (Table 1). Of the 13 animals,

R5, B3, B4, and B5, the first to develop moderately advanced tumors (Fig. 3A, left), were subjected to FDG-PET. This method allows detection of areas of high glucose consumption [6], and when carried out before and after treatment with 3-BrPA can help assess the extent of metabolic impairment. Trans-axial FDG-PET images (Fig. 3B) of tumors in the upper backs of R5, B3, B4, and B5 prior to treatment with 3-BrPA showed a localized region (“yellow” on the pseudo signal intensity bar in Fig. 1A, right) indicative of increased glucose consumption. In sharp contrast, after a 12 day period in which 3-BrPA was injected directly into the tumor site of each animal on eight different days causing tumor regression and disappearance, the resultant FDG-PET analyses showed no abnormal glucose consumption. Region of interest analysis of those images showed a measurable decrease in glucose consumption by the tumor. Taking all four animals, the decrease in tumor/background radioactivity was significant between the pre- and post-treatment scans ($P = 0.012$). Moreover, there has been no tumor recurrence for >7 months (see also [Supplementary material](#)).

All advanced solid tumors (HCCs) growing in the upper backs of test animals also regressed and disappeared following treatment with 3-BrPA

The remaining nine animals in Group 2 (B1, B2, B6, R1, R2, R3, R4, R6, and Sweetie) provided the greatest therapeutic challenge as tumors in each became advanced, i.e., ~3 cm (maximal dimension) and tended to spread to one of the front limbs (Fig. 3C, center, and human equivalent, left). Because of the aggressiveness of these tumors, several treatment approaches with 3-BrPA were investigated (Table 1). Regardless of the approach, further growth of each tumor in the nine animals was arrested, and over a 2–4 week period tumors in all animals regressed and disappeared (Fig. 3C, right, as one example). For >7 months there has been no recurrence (see also [Supplementary material for additional examples](#)).

In summary, advanced cancers growing either internally or externally were eradicated in all 19 treated animals using a simple unique ATP depletion strategy, thus providing “proof of principle” that it is possible to defeat quite vicious cancers and spare life at the edge.

Acknowledgments

Drs. Paul Talalay and Donald Coffey are acknowledged for valuable discussions and James Fox and David Blum for technical assistance. Y.H.K. is grateful also to Ilona McClintick and Dr. Ann Morrill for encouragement.

Appendix. Supplementary material

Supplementary data associated with this article can be found, in the online version, at [doi:10.1016/j.bbrc.2004.09.047](https://doi.org/10.1016/j.bbrc.2004.09.047).

References

- [1] J. Bruix, L. Boix, M. Sala, J.M. Llovet, Focus on hepatocellular carcinoma, *Cancer Cell* 5 (2004) 215–219.
- [2] O. Warburg, *The Metabolism of Tumors*, Arnold Constable, London, 1930.
- [3] P.L. Pedersen, Tumor mitochondria and the bioenergetics of cancer cells, *Prog. Exp. Tumor Res.* 22 (1978) 190–274.
- [4] P.L. Pedersen, S. Mathupala, A. Rempel, J.F. Geschwind, Y.H. Ko, Mitochondrial bound type II hexokinase: a key player in the growth and survival of many cancers and an ideal prospect for therapeutic intervention, *Biochim. Biophys. Acta* 1555 (2002) 14–20.
- [5] S. Yasuda, S. Arai, A. Mori, N. Isobe, W. Yang, H. Oe, A. Fujimoto, Y. Yonenaga, H. Sakashita, M. Imamura, Hexokinase II and VEGF expression in liver tumors: correlation with hypoxia-inducible factor 1 alpha and its significance, *J. Hepatol.* 40 (2004) 117–123.
- [6] E.M. Rohren, T.G. Turkington, R.E. Coleman, Clinical applications of PET in oncology, *Radiology* 231 (2004) 305–332.
- [7] E. Bustamante, P.L. Pedersen, High aerobic glycolysis of rat hepatoma cells in culture: role of mitochondrial hexokinase, *Proc. Natl. Acad. Sci. USA* 74 (1977) 3735–3739.
- [8] D.F. Smith, E.F. Walborg Jr., J.P. Chang, Establishment of a transplantable ascites variant of a rat hepatoma induced by 3'-methyl-4-dimethylaminoazobenzene, *Cancer Res.* 30 (1970) 2306–2309.
- [9] K. Shimoji, L. Ravasi, K. Schmidt, M.L. Soto-Montenegro, T. Esaki, J. Seidel, E. Jagoda, L. Sokoloff, M.V. Green, W.C. Eckelman, Measurement of cerebral glucose metabolic rates in the anesthetized rat by dynamic scanning with 18F-FDG, the ATLAS small animal PET scanner, and arterial blood sampling, *J. Nucl. Med.* 45 (2004) 665–672.
- [10] S. Siegel, J.J. Vaquero, L. Aloj, J. Seidel, W.R. Gandler, M.V. Green, Initial results from a PET/planar small imaging system, *IEEE Trans. Nucl. Sci.* 46 (1999) 571–575.
- [11] R. Yao, J. Seidel, C.A. Johnson, M.E. Daube-Witherspoon, M.V. Green, R.E. Carson, Performance characteristics of the 3-D OSEM algorithm in the reconstruction of small animal PET images. Ordered-subsets expectation-maximization, *IEEE Trans. Med. Imaging* 19 (2000) 798–804.
- [12] R. Hebel, M.W. Stromberg, *Anatomy of the Laboratory Rat*, Williams and Wilkins, Baltimore, 1976.
- [13] Y.H. Ko, B.A. McFadden, Alkylation of isocitrate lyase from *Escherichia coli* by 3-bromopyruvate, *Arch. Biochem. Biophys.* 278 (1990) 373–380.
- [14] Y.H. Ko, P.L. Pedersen, J.F. Geschwind, Glucose catabolism in the rabbit VX2 tumor model for liver cancer: characterization and targeting hexokinase, *Cancer Lett.* 173 (2001) 83–91.
- [15] J.F. Geschwind, Y.H. Ko, M.S. Torbenson, C. Magee, P.L. Pedersen, Novel therapy for liver cancer: direct intraarterial injection of a potent inhibitor of ATP production, *Cancer Res.* 62 (2002) 3909–3913.